



## Folate targeting of drug carriers: A mathematical model

Ketan B. Ghaghada<sup>a,b</sup>, Justin Saul<sup>d,e</sup>, Jayaganesh V. Natarajan<sup>b,c</sup>,  
Ravi V. Bellamkonda<sup>d,e</sup>, Ananth V. Annapragada<sup>a,b,\*</sup>

<sup>a</sup>Department of Chemical Engineering, University of Houston, Houston, TX, United States

<sup>b</sup>School of Health Information Sciences, University of Texas-Houston Health Science Center, Houston, TX, United States

<sup>c</sup>Graduate School of Biomedical Sciences, University of Texas-Houston, Houston, TX, United States

<sup>d</sup>Wallace H. Coulter Department of Biomedical Engineering, Georgia Institute of Technology/Emory University, Atlanta, GA, United States

<sup>e</sup>Department of Biomedical Engineering, Case Western Reserve University, Cleveland, OH, United States

Received 21 September 2004; accepted 23 January 2005

Available online 13 March 2005

### Abstract

The binding of folate-targeted drug carriers to a receptor-bearing cell surface is modeled using a deterministic approach. The model accounts for the presence of multiple folate ligands on the carrier surface, the anchoring and presentation of the ligands on flexible polymeric tethers, and the combination of both clustered and homogeneous spatial distributions of receptors on the cell surface. The model was validated against an experimental system where folate-bearing liposomes were used as delivery vehicles to deliver drug to tumor cells *in vitro*. Unknown parameters of the model were then estimated by a least-squares fit to the experimental data. A parametric study systematically varying the estimated parameters around the best-fit values indicated that the model was sensitive to these parameters, lending credence to their estimated values. This study indicates that drug uptake is dependent on several factors including the ligand number, the exposure time, and carrier concentration. For the specific case of folate targeting, the cumulative uptake of folate ligands is important, causing a decrease in the carrier uptake rate once a threshold cumulative uptake is crossed.

© 2005 Published by Elsevier B.V.

**Keywords:** Receptor; Ligand; Tethered ligands; Targeted drug delivery; Ligand-bearing carriers; Mathematical model; Receptor distribution; Carrier–cell interactions

### 1. Introduction

Current efforts to selectively deliver chemotherapeutic agents to their sites of action have focused on exploiting the natural endocytosis pathway by targeting an over-expressed receptor or antigen on the surface of target cell. Receptor-mediated targeting of

\* Corresponding author. School of Health Information Sciences, University of Texas-Houston Health Science Center, 7000 Fannin Street, Suite 600, Houston, TX 77030. Tel.: +1 713 500 3982; fax: +1 713 500 3907.

E-mail address: [Ananth.Annapragada@uth.tmc.edu](mailto:Ananth.Annapragada@uth.tmc.edu) (A.V. Annapragada).

long circulating carriers has been accomplished by attachment of ligands to the distal end of the polymer chains. Interaction between the targeting ligands and the cell surface receptors allows the carrier to be bound to the cell surface for a time sufficient to facilitate internalization of the vehicle and the drug that it contains. A number of ligand-presenting delivery systems targeting differentially expressed receptors on tumor cells have been studied to promote increased drug uptake [1–5].

Substantial progress has been made in understanding ligand–receptor interactions [6–9], and cell–cell interactions [10,11]. Models of cell–surface interactions at steady state [12,13], steric effects arising from the receptor size/spacing and multivalent ligands [14] and receptor/ligand clustering have been studied [15].

Drug carrier–cell interactions, however, are fundamentally different from cell–surface interactions since the drug carrier is approximately two orders of magnitude smaller in size than the cell, increasing the role of surface curvature in the binding process. Existing drug carrier targeting models are limited to monovalent interactions, and do not address many of the physical phenomena that arise from surface curvature and multivalency/polyvalency [16,17].

Virus–cell binding has been modeled recently [18] and this model accounts for the steric effects due to virus size, which is comparable to the size of a drug carrier, as well as the distribution of rigidly attached binding sites on the surface of the virus. However, in being faithful to the anatomy of a typical virus, the binding ligands are assumed to be at the surface of the virus. Therefore, there is no consideration given to possible effects of tethering of the ligands on the carrier surface, for example by flexible polymer chains. Drug carriers however, do use such tethers since targeting efficiency is greatly increased by the presence of such tethers (the increase in spatial freedom afforded to the tethered ligands, approximates the reactivity of the free ligand molecule).

Ultimately, one concludes that the current literature does not present a model that takes into account the steric effects of ligand/receptor clustering, flexible ligand tethers, multivalent/polyvalent interactions and carrier:cell size ratio that characterize targeted drug

delivery systems. The current work was therefore directed at developing such a model.

Specifically, the physical system studied is the targeting of liposomes to C6 glioma and KB cells via the folate receptor. Experimental studies done previously have shown that liposome uptake increased with the number of folates per liposome, until a threshold was reached, after which the uptake dropped [19]. A possible explanation for this behavior is the regulation of the folate receptor cycle by the intracellular folate demand [20]. The mathematical model developed in this paper therefore includes this regulation, and is validated against the experimental data. A numerical sensitivity analysis was also performed on the model to gain additional insights into the transient behavior of the system.

## 2. Theory

A number of factors govern the interaction of tethered ligands on the surface of carrier and receptors on the surface of cell. It has been shown that the distance of separation between two curved surfaces plays a significant role in the binding of tethered ligand and receptor [21]. As the two surfaces approach each other, the overall free energy of the system starts decreasing as a result of binding between the receptors and ligands. At a certain critical distance the overall free energy of the system reaches a minimum, coincident with the onset of spontaneous contact. It was also shown that for a ligand–receptor pair having a high association constant, the vast majority of ligand–receptor bond formation will take place at this critical distance, also defined as the binding distance. At a binding distance separation between the carrier and the cell surface, the number of bonds that can be formed will therefore depend on 1) number of ligands on the surface of carrier, 2) length of tether, 3) carrier size, and 4) receptor density on the surface of cell. Thus, based on a given receptor density and distribution, carriers can be tailored (by altering the tether length and number of ligands) to achieve optimal binding to the cell.

To study the effect of carrier diameter and tether length on carrier binding, two quantities that accounted for carrier–cell interactions were calculated.

### 2.1. Active fractional area of carrier (AFAC)

The active fractional area of carrier is defined as the fraction of carrier surface that is available for binding to the cell. The AFAC is a function of tether size, ligand size and carrier size. Fig. 1 illustrates the interactions between a carrier and a cell. Assume that the separation distance between the carrier and receptors on the surface of cell is equal to the binding distance [21]. Thus varying the tether length alters the binding distance between the carrier and cell surface receptors since binding distance is a function of tether length. Therefore, the separation distance is a function of tether length. Further, assume that the tether at the outermost end of the AFAC forming a receptor–ligand complex is in a fully extended conformation. Therefore using simple geometry, the active fractional area of carrier is given by

$$A_{\text{AFAC}} = 2\pi RH / 4\pi R^2 \quad (1)$$

This can be simplified further to give

$$A_{\text{AFAC}} = H / D_C \quad (2)$$

where  $R$  is the radius of the carrier and  $D_C$  is the diameter of the carrier.  $H$  is given by  $(L - d_B)$  when  $L \leq (R + d_B)$ . Here,  $L$  corresponds to the sum of ligand length and the maximum extended length of the tether;  $d_B$  is the binding distance. However, when  $L > (R + d_B)$ , the fully extended tether is able to reach beyond the projected carrier surface. By assuming that

the tether becomes tangent to the carrier surface for forming a receptor–ligand complex the definition for  $H$  becomes  $(R + x)$ , where  $x$  is the vertical distance above the horizontal line passing through the center of the carrier as defined in Fig. 1. It indicates the position of the fully extended tether on the carrier surface that is both tangent to the surface of the carrier and reaching the cell surface. Fig. 2 shows a plot of AFAC as a function of PEG molecular weight for different carrier sizes. Therefore based on the AFAC, the number of ligands available for binding can be calculated. The choice of binding distance as the distance at which the calculations were done was based on the fact that maximum number of bonds between the carrier and cell surface occurs at this distance [21]. Thus the majority of the carriers bound to the cell are expected to be found at this distance at any point in time.

### 2.2. Area of influence (AOI)

The number of receptors that are accessible to a carrier depends on the area covered by the tether on the surface of cell. The area of influence (AOI) is defined as the maximum area that a carrier can cover on the surface of cell depending on the length of tether and carrier size. The area of influence can be calculated by assuming that the tether that reaches the furthest on the surface of cell will be fully extended. Fig. 3 shows a plot of the dependence of

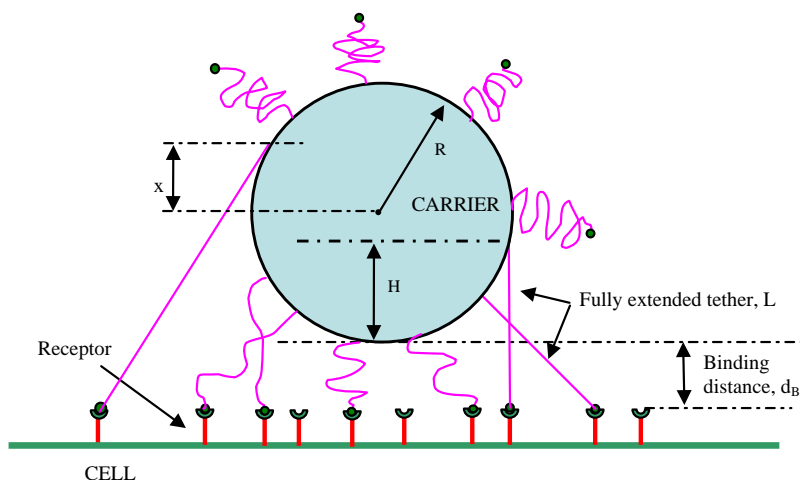


Fig. 1. Schematic illustration of carrier–cell interactions.

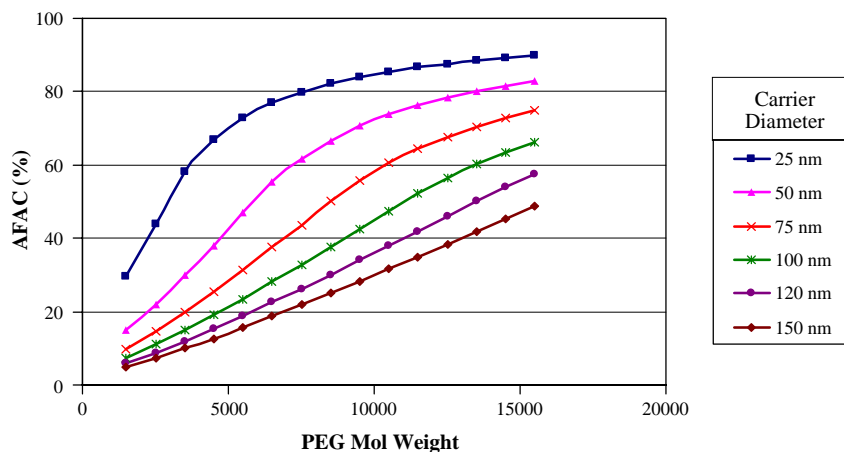


Fig. 2. Active fractional area of carrier, (AFAC), as a function of PEG molecular weight for different carrier sizes.

AOI as a function of PEG molecular weight for different carrier sizes. Therefore, based on a given receptor density and distribution, the number of receptors accessible to a carrier can be calculated using the area of influence.

### 2.3. Internalization of folate-bearing drug carriers

Ligand-bearing drug carriers enter the cell through receptor-mediated endocytosis, a process which involves binding of ligand-bearing carriers with receptors expressed on the surface of the cell followed by internalization of the complex. Lipid rafts repre-

sents the major pathway for internalization of many glycosylphosphatidylinositol-anchored (GPI) proteins. The rafts are normally 50–300 nm in size and comprise a minor fraction of the cell membrane [23–25]. Folate receptor, a GPI-anchored protein over-expressed on a number of cancer cells is internalized through this pathway [26]. Several studies have shown that GPI-anchored proteins are found to be clustered in specialized lipid rafts called microdomains [24,27, 28]. It has been reported that GPI-anchored folate receptors are clustered in microdomains of around 70 nm in size containing approximately 50 folate receptors [24].

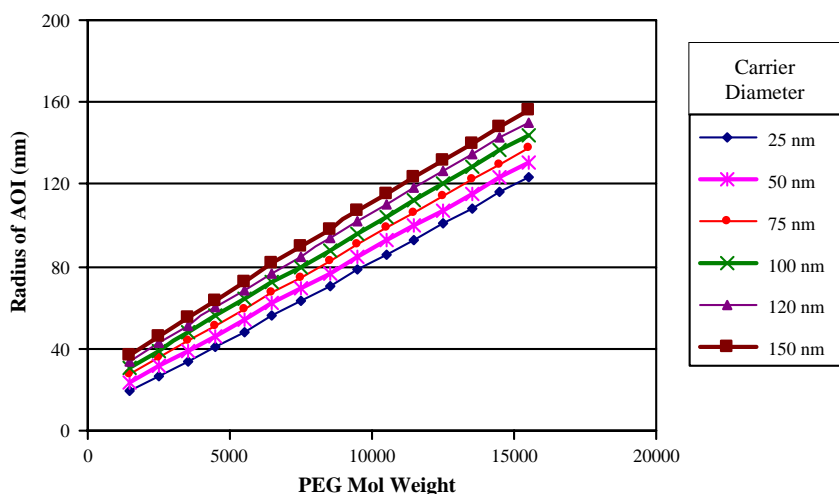


Fig. 3. Area of influence, (AOI), as a function of PEG molecular weight for different carrier sizes.

Several drug carriers targeting the folate receptor have been studied [2,5,29]. However, none of the studies published have accounted for the spatial distribution of receptors in designing optimal drug carriers. For instance, one would envision that folate-bearing carriers that target cancer cells over-expressing folate receptors should be designed such that sufficient numbers of carriers bind on the cell surface to allow increased numbers of carriers to be internalized. Thus in the case of C6 and KB cell lines which both express folate receptors, one could hypothesize that an optimal design of the targeted liposomes would be such that each liposome binds to a single cluster. Therefore, depending on the density and distribution of receptors, one could design the targeted carrier to have an optimum tether length and an optimum number of ligands to allow the carrier to form sufficient bonds with receptors on the surface to prevent detachment and thus gain entry into the cell.

### 3. Model development

A detailed description of the experimental methods and materials used to study the uptake of folate-bearing liposomes by tumor cells has not been presented here since it has already been described elsewhere [19]. Briefly, liposomes bearing different number of folate ligands attached to the extremity of PEG were formulated. These carriers were loaded with an anti-cancer drug, doxorubicin. Cell culture medium containing the folate-bearing liposomes was incubated with tumor cells for 2 h in 35 mm diameter wells. The numbers of cell-associated liposomes were estimated by fluorescence measurement of the doxorubicin and the calculation of the corresponding amount of phospholipids.

A population balance deterministic model was developed to study the uptake of drug carriers by cells in vitro. While the binding phenomenon encountered in this process is relatively fast, and 2–4 h is a sufficiently long time to result in equilibration, the addition of receptor-mediated internalization adds a long time scale to the overall process. Unfortunately, as demonstrated in this paper, this long time scale does not always manifest itself in the experimental data due to the confounding effects of receptor down-regulation. That an equilibrium model was inadequate

to model this process became apparent when it was unable to fit the experimental data. Therefore a kinetic model that included two key phenomena relevant to the system was chosen. The phenomena considered in this model were: 1) binding of carriers to the surface of the cell, and 2) internalization of carriers into the cell through receptor-mediated endocytosis. Since the interaction between the targeted carrier and cell surface occurs through receptor–ligand bond formation, the basis of interaction for developing the model is the receptor–ligand interaction. Since folate receptors are clustered on the cell surface, the distance between the centers of any two adjacent clusters, also defined as the inter-cluster spacing, determines the number of clusters available for interaction with a single carrier. However, to our knowledge, there is no literature available on the distribution of folate clusters on the cell surface. Since the number of folate receptors per cluster may vary from cluster to cluster, an average value for the number of clusters was calculated using the relation

$$C = N_T/N_C \quad (3)$$

where,  $C$  is the average number of clusters on the cell surface;  $N_T$  is the total number of surface receptors per cell;  $N_C$  is the total number of receptors per cluster on the surface. Further, assume that the clusters are uniformly distributed on the surface of the cell. Based on the total number of surface folate receptors quantified in the experimental study [19] (280,000 surface folate receptors per cell for KB cells and 10,000 surface folate receptors per cell on C6 cells), the inter-cluster spacing was calculated to be 1120 nm for C6 cells and 209 nm for KB cells. For the 2000 molecular weight PEG used in the experimental study, the tether length is 15.8 nm, and yields an AOI of 65 nm radius. Since the diameter of a cluster of folate receptors is 70 nm, it is therefore apparent that only one cluster is accessible by each liposome.

The species formed on the surface, as a result of the multivalent interactions of the carrier with the surface are modeled by a population balance formalism. Let  $C_{Car}$  denote the concentration of free carrier in the solution, mol/cm<sup>3</sup>. Let  $C_{clus,surf}$  denote the surface concentration of clusters present on the surface of a cell, mol/cm<sup>2</sup>. The surface concentration of bound carrier attached through  $i$  bonds is denoted by  $x_i$ , mol/cm<sup>2</sup>. Let  $a$  denote the total number of ligands per

carrier and  $b$  denote the total number of receptors per cluster. The mass balance equation for  $C_{\text{Car}}$  gives

$$dC_{\text{Car}}/dt = - \{k_f^v \{aC_{\text{Car}}\} \{bC_{\text{clust,surf}}\} - k_r^v x_1\} Z \quad (4)$$

where,  $k_f^v$  is the binding rate constant on volume basis,  $\text{cm}^3/\text{mol}/\text{min}$ ;  $k_r^v$  is the dissociation rate constant on volume basis,  $1/\text{min}$ ;  $Z$  is a factor that converts the volume concentrations to appropriate cell surface concentrations,  $\text{cm}^2/\text{cm}^3$ .  $Z$  is defined as the product of cells per unit volume times the area of a cell.

The balance for carriers bound through one bond,  $x_1$  gives

$$dx_1/dt = k_f^a \{aC_{\text{Car}}\} \{bC_{\text{clust,surf}}\} - k_r^v x_1 - k_f^a \{(w-1)x_1\} \{(r-1)x_1\} + 2k_r^a x_2 - k_{\text{in}} x_1 \quad (5)$$

where,  $k_f^a$  is the 2-D binding rate constant,  $\text{cm}^2/\text{mol}/\text{min}$ ;  $k_r^a$  is the 2-D dissociation rate constant,  $1/\text{min}$ ;  $k_{\text{in}}$  is the internalization rate constant for folate receptors,  $1/\text{min}$ ;  $w$  is the the number of ligands per carrier available for bond formation based on AFAC; and  $r$  is the number of receptors per cluster available for bond formation based on AOI. The first term on the R.H.S refers to the reaction between free active ligands on carriers and free active receptors in clusters on the cell surface. The factor of 2 in the fourth term on the R.H.S is present to account for statistical factors i.e., a carrier bound by 2 bonds can dissociate to form a carrier bound by one bond in two distinct ways: the dissociation of either of the original bonds. The third term on the R.H.S represents interaction between a carrier with  $(w-1)$  active unbound ligands and a cluster with  $(r-1)$  active unbound receptors. The last term accounts for the internalization of the carrier–cluster complex into the cell. The 2-D rate constants can be calculated using the linear relation [30]

$$K_v = sK_a \quad (6)$$

where,  $K_v$  is the 3-D equilibrium constant,  $\text{mol}/\text{cm}^3$ ;  $K_a$  is the 2-D equilibrium constant,  $\text{mol}/\text{cm}^2$ ; and  $s$  represents the length defining the region where reaction becomes possible,  $\text{cm}$ . For our system, since

the ligand is attached to the distal end of the tether,  $s$  is defined as the fully extended length of the tether.

Similarly, the balance for carriers bound through  $i$  bonds gives

$$dx_i/dt = k_f^a \{(w-(i-1))x_{i-1}\} \{(r-(i-1))x_{i-1}\} + (i+1)k_r^a x_{i+1} - k_f^a \{(w-i)x_i\} \{(r-i)x_i\} - ik_r^a x_i - k_{\text{in}} x_i \quad \text{for } i = 2, \dots, n-1 \quad (7)$$

where,  $n$  is the maximum number of bonds a carrier can form. The value of  $n$  is equal to the minimum of either  $w$  or  $r$ . A balance for carriers bound through  $n$  bonds gives

$$dx_n/dt = k_f^a \{(w-(n-1))x_{n-1}\} \{(r-(n-1))x_{n-1}\} - nk_r^a x_n - k_{\text{in}} x_n. \quad (8)$$

The balance for free clusters on the surface of the cell gives

$$dC_{\text{clust,surf}}/dt = -k_f^v \{aC_{\text{Car}}\} \{bC_{\text{clust,surf}}\} + k_r^v x_1 - k_{\text{in}} C_{\text{clust,surf}} + k_{\text{out}} C_{\text{clust,int}} \quad (9)$$

where,  $k_{\text{out}}$  is the externalization rate constant for folate receptors,  $1/\text{min}$ ; and  $C_{\text{clust,int}}$  is the intracellular concentration of clusters,  $\text{mol}/\text{cm}^2$ . A cluster on the surface can therefore have four states: 1) bound state if a carrier is attached to it, 2) unbound state if there is no carrier attached to it, 3) internalization state if the cluster is in the process of undergoing internalization, 4) externalization state if a new cluster is being formed due to transport of folate receptors onto the surface. The balance for receptors on the cell surface gives

$$dC_{\text{receptor}}/dt = -k_f^v \{aC_{\text{Car}}\} \{bC_{\text{clust,surf}}\} + \sum_{j=1}^n (jk_r^a x_j - bk_{\text{in}} x_j) - \sum_{j=1}^{n-1} k_f^a \{(w-j)x_j\} \{(r-j)x_j\} - k_{\text{in}} b C_{\text{clust,surf}} + k_{\text{out}} b C_{\text{clust,int}}. \quad (10)$$

A balance on the internalized clusters gives

$$dC_{\text{clust,int}}/dt = \sum_{j=1}^n (k_{\text{in}} x_j) + k_{\text{in}} C_{\text{clust,surf}} - k_{\text{out}} C_{\text{clust,int}}. \quad (11)$$

Finally the balance for internalized carriers gives

$$dC_{\text{Car,int}}/dt = \sum_{j=1}^n (k_{\text{in}}x_j). \quad (12)$$

Upon the introduction of appropriate values for the rate constants and a vector of initial conditions, the system of ordinary differential equations can be integrated to obtain time-varying concentration of various species formed in the system. A summation of the number of carriers internalized and the total number of surface bound carriers would then provide the total number of carriers associated with each cell.

### 3.1. Choice of parameters

Folic acid has a high affinity for the  $\alpha$ -folate receptor with an *equilibrium dissociation constant* of  $10^{-10}$  M [22,29,31]. However, to our knowledge, there is no data available on the individual *rate constants* for folic acid ligand– $\alpha$ -folate receptor system. In the current model, the rate constants were therefore calculated using the best fit to the experimental data obtained previously [19]. In this fitting process, the ratio of binding rate constant to dissociation rate constant was constrained to be equal to the overall equilibrium dissociation constant obtained from the literature.

The regulation of folate receptor under conditions in which cellular demands for folates are altered has been studied by measuring the folate receptor function and levels in cells with different growth rates [20]. It was found that the folate receptor function is regulated by cellular requirements for folates. A down-regulation of folate receptor function was observed in response to a decreased need for folic acid for cell growth. Consequently, once a certain amount of folic acid required for cell growth is achieved, the cell signals a significant slowdown of the receptor trafficking cycle. Quantitatively, this results in a decrease in the internalization and the externalization rate constants for folate receptor, thus inhibiting uptake of folate-bearing liposomes. The threshold intracellular concentration is defined as the concentration of folic acid in the cell at which the down-regulation of folate receptor commences. In another study, it was found that KB cells internalized approximately  $2 \times 10^7$  folate conjugates per cell

before receptor down-regulation occurred [32]. To our knowledge, there have been no studies conducted on measuring the internalization and externalization rates of folate receptors during down-regulation of folate receptors. In our model the down-regulation of the folate receptor cycle is approximated by a decrease in the value of the rate constants. Hence, after the threshold concentration of folic acid is reached, the internalization and externalization rate constants for folate receptor are approximated to be inversely proportional to the intracellular folic acid concentration, defined by the following equations:

$$k'_{\text{in}} = k_{\text{in}} \frac{1}{(C_{\text{F}} * t)} \quad (13)$$

$$k'_{\text{out}} = k_{\text{out}} \frac{1}{(C_{\text{F}} * t)} \quad (14)$$

where,  $k'_{\text{in}}$  is the internalization rate constant during the down-regulation phase, 1/min;  $k_{\text{in}}$  is the internalization rate constant during the normal uptake phase, 1/min;  $k'_{\text{out}}$  is the externalization rate constant during the down-regulation phase, 1/min;  $k_{\text{out}}$  is the externalization rate constant during the normal-uptake phase, 1/min;  $C_{\text{F}}$  is the intracellular folic acid concentration, molecules per cell; and  $t$  is the incubation time, min.

The ratio of number of intracellular folate receptors to the number of folate receptors on the surface depends on the growth requirements of the cell [20,31,33,34]. In our model, the ratio was set to unity based on data available in the literature [31,34]. For the model, the total number of folate receptors present on the surface of C6 glioma cells and KB cells, as quantified in the experimental study [19], were  $9.7 \times 10^3$  and  $2.8 \times 10^5$ , respectively.

Using fluorescence resonance energy transfer (FRET) microscopy, it was shown that folate receptors are clustered in microdomains on the surface of CHO cells [24]. These microdomains are approximately 70 nm in size, each containing fewer than 50 folate receptors. In another study, chemical cross-linking was used to show that microdomains of GPI-anchored proteins exist on the surface of living cells with approximately 15 molecules per microdomain [27]. Intracellular concentration of folic acid varies with

different cell line due to different growth requirements. No reference to the normal levels of folic acid in KB or C6 cell lines exists in the literature. However, the intracellular concentration of folates in MA104 cell line grown under folate-deficient medium is approximately  $3 \times 10^5$  molecules per cell [33]. A value of  $5 \times 10^5$  was used as the initial intracellular folic acid for the model. A tether length of 15.75 nm corresponding to the fully extended PEG-2000, used in the experimental study [19], was considered in the model.

### 3.2. Method of solution

The resulting non-linear first order ordinary differential equations (ODEs) were solved numerically using DVODE implemented in FORTRAN [35]. The number of ODEs in the system varied from 20 to 70 depending on the number of receptors per cluster. While it would have been preferable to parameterize this model and identify governing dimensionless groups, the population balance formalism used for the polyvalent binding makes it difficult to do so. Therefore numerical parametric variations were performed to probe the model.

As described in the previous section, several parameter values were unavailable for the given system. The DVODE numerical integrator was therefore combined with a Levenberg–Marquardt (L–M) routine. This routine iterated the following parameters; binding rate constant ( $k_f$ ), number of folate receptors per cluster ( $b$ ), internalization rate constant ( $k_{in}$ ), and externalization rate constant ( $k_{out}$ ) to achieve the best possible fit of the DVODE solution to the data obtained in the experimental study [19]. A relative difference in the  $\chi^2$  value of less than 0.01 was used as the convergence criteria for the L–M method. The parameter set that resulted in the best fit was verified to be physically meaningful. For instance, the binding and the dissociation rate constants for the receptor–ligand pair was compared with the general range in which the rate constants for a majority of receptor–ligand pair are known to exist [10]. The number of folate receptors per cluster was compared to the range mentioned in the literature [24,27]. The externalization and the internalization rates were compared to values available in the literature for other cell lines [34].

## 4. Results

### 4.1. Liposome uptake in C6 and KB cells

In the experimental study, the non-specific uptake obtained with non-targeted liposomes in C6 cells was significant compared to the uptake observed with folate-targeted liposomes. Since the current model was based on studying the uptake due to receptor-mediated endocytosis, the non-specific uptake was subtracted from the uptake observed with folate-targeted liposomes. Fig. 4 shows the comparison of specific uptake calculated from the experimental data versus the simulation results for liposome uptake in C6 cells. Initially, the liposome uptake increases with an increase in the number of ligands per liposome. However, once the number of ligands per liposome reaches approximately 500, there is a decrease in liposome uptake with an increase in number of ligands per liposome.

For KB cells, the non-specific uptake was negligible compared to the specific uptake observed with folate-targeted liposomes. Fig. 5 shows the comparison of experimental data with the simulated data for liposome uptake in KB cells. Again, after the initial increase in uptake with number of ligands, the uptake levels off and then drops. The drop off occurs at around 700 ligands per liposome compared to 500 for C6 cells. This drop off is consistent with the fact that at higher ligand numbers the overall uptake of liposomes is limited by the internalization/externalization rates of folate receptors which controls the entry of folate bound liposomes into the cell. The internalization/externalization rates in turn depend on the cellular demand for folate. Thus the down-regulation of the folate receptor cycle is initiated at lower number of liposomes per cell due to the uptake of larger amounts of folic acid. A similar phenomena was observed in another study where liposomes containing fewer folate ligands per liposome (<0.3 mol%) yielded higher binding efficiencies compared to liposomes containing higher number of folic acid per liposome [36].

### 4.2. Parametric analysis

In order to understand the range of behavior that can be represented by this model, it was numerically solved over a range of parameters. Fig. 6 shows the

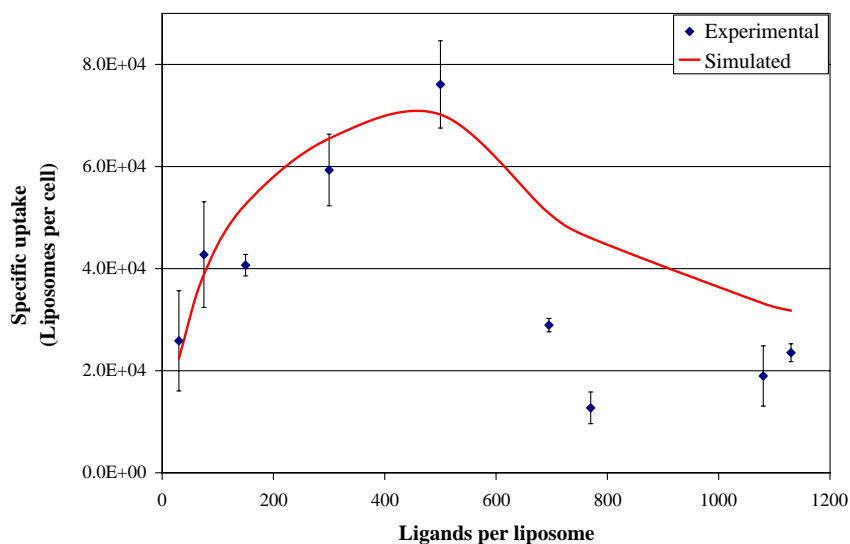


Fig. 4. Comparison of experimental data with simulated data for C6 cell culture experiment. The specific uptake is calculated by subtracting the non-specific uptake obtained with non-targeted liposomes from uptake obtained with folate-targeted liposomes. The uptake obtained with folate-targeted liposomes, which comprises of liposomes bound on the surface and liposomes internalized, was calculated as a function of number of ligands per liposome.

predicted effect of incubation time on liposome uptake in C6 cells. An increase in liposome uptake is observed with increasing incubation time. However this behavior is observed only for cases where the number of ligands per liposome is still low enough that folate receptor cycle down-regulation is not triggered. The peak value for the number of liposomes

per cell shifts to lower ligand numbers as the incubation time is increased. This is due to the fact that the predicted intracellular folic acid ligand concentration has not reached the threshold value at these low ligand numbers, thus allowing a continued uptake of liposomes. The majority of the cell-based uptake experiments in the literature use an incubation

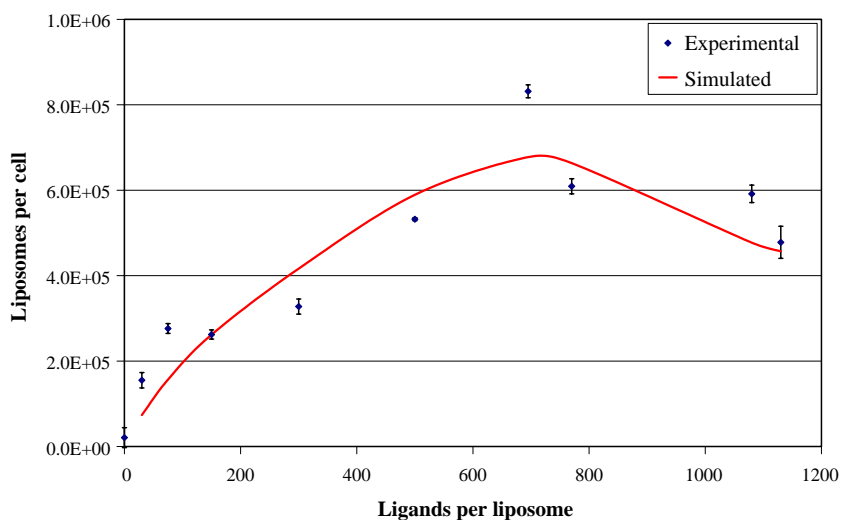


Fig. 5. Comparison of experimental data with simulated data for KB cell culture experiment. The number of liposomes per cell, which comprises of liposomes bound on the surface and liposomes internalized, was calculated as a function of number of ligands per liposome.

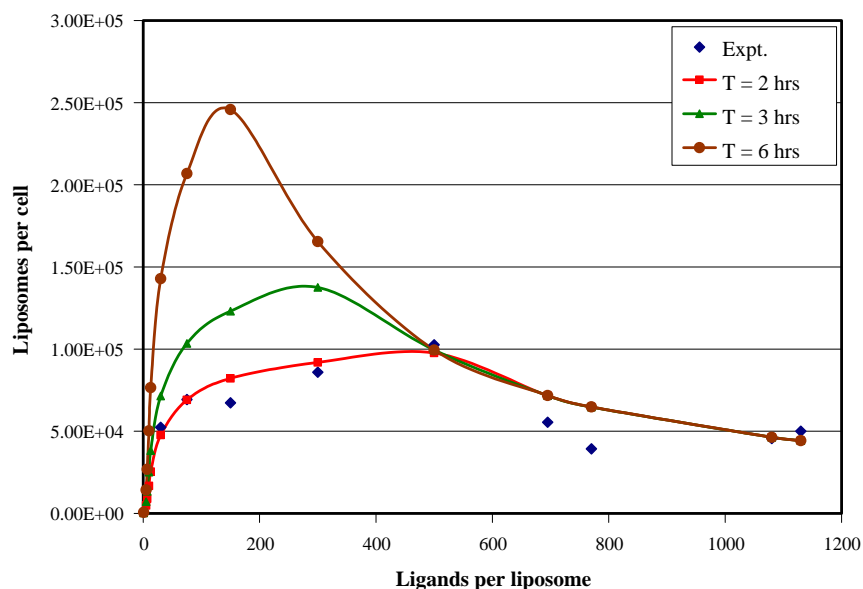


Fig. 6. Predicted effect of incubation time on liposome uptake in C6 cells. The number of liposomes per cell, which comprises of liposomes bound on the surface and liposomes internalized, was calculated as a function of number of ligands per liposome.

time of 4–6 h and it is usually assumed that equilibrium has been achieved by this time. It is apparent however, that the uptake system is far from equilibrium at low folates per liposome. At higher folates per liposome, equilibrium is indeed reached

since the uptake is now governed by the uptake rate and not the binding.

Fig. 7 shows the predicted effect of liposome concentration on liposome uptake in C6 cells. At low ligand numbers per liposome, an increase in liposome

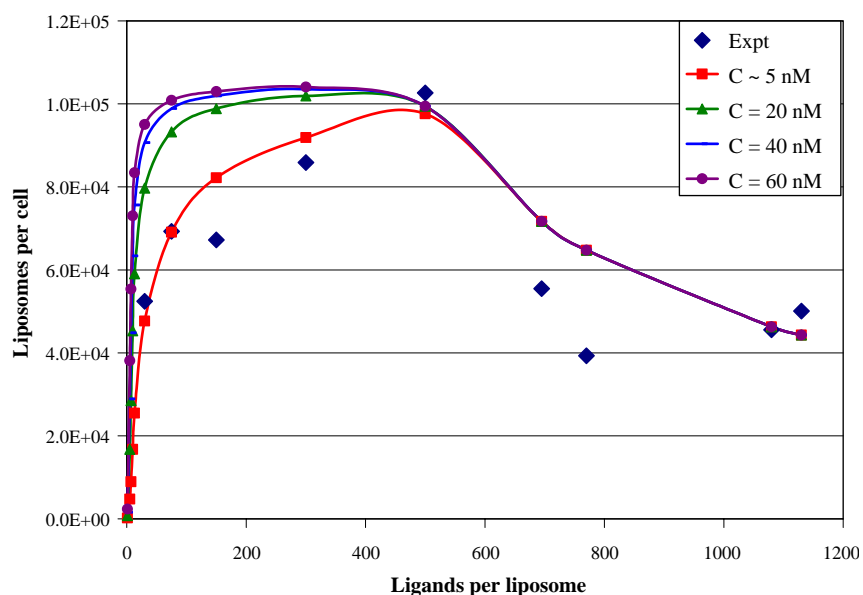


Fig. 7. Predicted effect of liposome concentration on liposome uptake in C6 cells. The number of liposomes per cell, which comprises of liposomes bound on the surface and liposomes internalized, was calculated as a function of number of ligands per liposome.

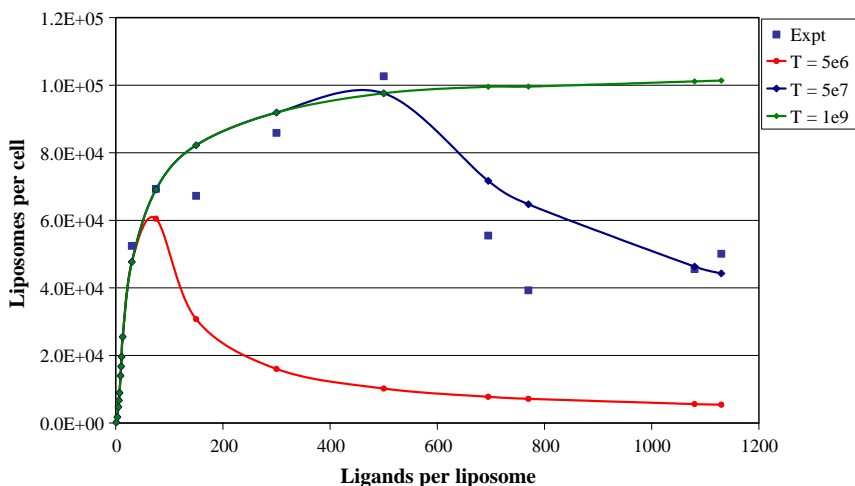


Fig. 8. Predicted effect of threshold intracellular folate concentration on liposome uptake in C6 cells. The threshold intracellular folate concentration is defined as the number of intracellular folic acid molecules per cell which when exceeded results in the down-regulation of folate receptor cycle. The number of liposomes per cell, which comprises of liposomes bound on the surface and liposomes internalized, was calculated as a function of number of ligands per liposome.

concentration results in an increase in uptake. This is due to the fact that at low ligand numbers, the calculated intracellular folate concentration of the cell does not reach saturation. However, the maximum number of liposomes that can be internalized per cell is limited by the incubation time and the rate of binding and internalization.

Fig. 8 shows the predicted effect of threshold concentration on liposome uptake in C6 cells. At a

low threshold limit, the maximum uptake occurs at lower ligand numbers per liposome. Further, the down-regulation of receptor cycle occurs at lower number of ligands per liposome resulting in a far lower uptake for liposomes containing higher ligand numbers. An increase in the threshold limit results in an increase in liposome uptake up to a certain ligand number per liposome. Further increases in ligand number do not lead to higher liposome uptake by the

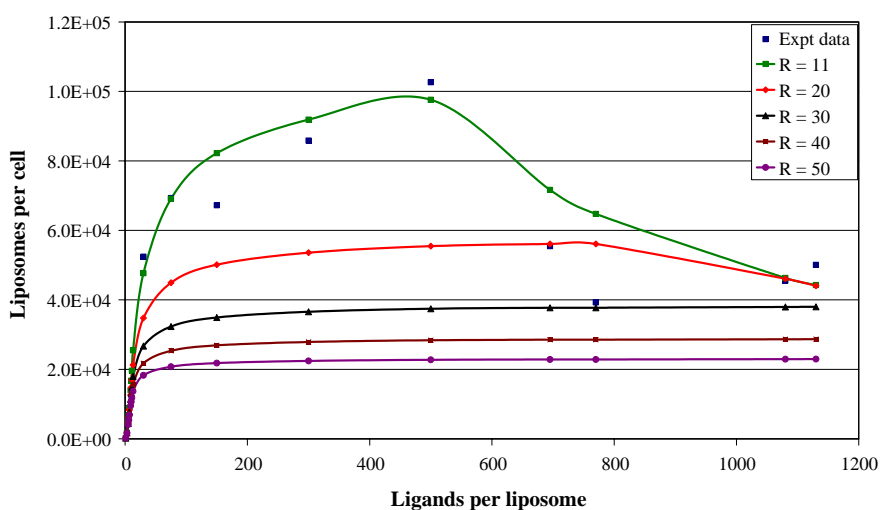


Fig. 9. Effect of number of receptors per cluster on liposome uptake in C6 cells. The number of liposomes per cell, which comprises of liposomes bound on the surface and liposomes internalized, was calculated as a function of number of ligands per liposome.

cells since the rate limiting step at this stage is the internalization rate of folate receptors. However, down-regulation of the folate receptor cycle is not reached since the threshold has been raised.

Fig. 9 shows the predicted effect of number of receptors per cluster on liposome uptake in C6 cells. An increase in the number of receptors per cluster results in a decrease in liposome uptake. This is due to the fact that at large number of receptors per cluster, the total number of clusters is reduced thus allowing fewer liposomes to internalize. Additionally, increasing the number of ligands per liposome does not increase the uptake due to the rate limiting internalization step. At higher receptors per cluster, the down-regulation of receptor cycle is also not triggered due to reduced liposome uptake.

## 5. Discussion

The purpose of this study was to develop a quantitative understanding of the interaction between ligand-bearing drug carriers and tumor cells to facilitate the design of optimal drug carriers. To model this physical system, an understanding of the process for interaction of carriers with receptors on the cell surface and the cell mechanisms for internalization of surface receptors and their associated complexes is critical. In this work, a deterministic model was developed to study the targeting of folate-bearing liposomes to tumor cells *in vitro*, based on the experimental work described elsewhere [19]. The current model was able to reasonably predict the behavior of the system. The uptake of folate-bearing liposomes differed considerably in C6 and KB cells lines (Figs. 4 and 5). Further, in both the cell lines the uptake of liposomes passes through a maximum, following which the liposomal uptake decreases with increasing ligand numbers. A possible explanation for the decrease in liposome uptake for very high ligand numbers is the down-regulation of the folate receptor function as studied by Doucette and Stevens [20]. They found that the folate receptor function is regulated by cellular folate requirements. Therefore, for carriers containing a large number of folic acid ligands, even a small amount of uptake is sufficient to trigger the down-regulation of the folate receptor cycle. The down-regulation will result in the slowing

down of the internalization/externalization rates of the receptor, consequently reducing liposome uptake. In the case of modeling the experimental data for C6 cell line, the non-specific uptake obtained with non-targeted liposomes was significant compared to uptake observed with folate-targeted liposomes. As a result, the non-specific uptake was subtracted from observed uptake with folate-targeted liposomes since it was assumed that the non-specific uptake is independent of the number of folate ligands attached to the liposome. The model was then used to fit the specific uptake data.

A comparison of the parameters obtained for the two cell lines are shown in Table 1. The binding rate constant for the folate receptor–ligand pair is different in the two cell types. This variation may be due to the difference in receptor distribution on the two cell types. In the current model, the distribution of clusters has been assumed to be uniform. Therefore the number of clusters on the surface of the cell, number of receptors per cluster and the inter-cluster spacing are calculated as average values. In reality these numbers may vary from cell to cell. This can alter the binding and internalization of liposomes on different cells. In addition to the receptor distribution, the binding of tethered folic acid ligand to folate receptors may also be affected by the dynamics of the tether. The variation in rate constants may also be due to differences in the structural isoforms found in the two cell types. Other studies have also shown that the structure of folate receptor is different on different cell types [37,38]. A pervasive theme in the literature is the consistent reporting of equilibrium binding constants for receptor–ligand interactions, but extremely few studies or reports of the rate constants (i.e. the on- and off-rates). A fundamental question is what the

Table 1  
Comparison of optimal parameter set for C6 and KB model

Parameter	Values for C6 model	Values for KB model
Binding rate constant (M min <sup>-1</sup> )	3.7010 * 10 <sup>5</sup>	1.5524 * 10 <sup>4</sup>
Dissociation rate constant (min <sup>-1</sup> )	3.7010 * 10 <sup>-5</sup>	1.5524 * 10 <sup>-6</sup>
Internalization rate constant (min <sup>-1</sup> )	0.6124	0.6295
Externalization rate constant (min <sup>-1</sup> )	0.1687	0.5784
Folate receptors per cluster	4	18
Threshold concentration (folic acid molecules per cell)	3.5 * 10 <sup>7</sup>	5 * 10 <sup>8</sup>

behavior of a receptor–ligand system that exhibits a particular equilibrium binding constant by virtue of specific on- and off-rates would be, compared to a different system that exhibits the same equilibrium binding constant by virtue of different on- and off-rates. An example from the field of leukocyte rolling would be the role of selectins vs. integrins, both of which have a high binding constant, but the selectins have higher on- and off-rates than the integrins [39]. The result in the leukocyte case of course, is that selectins mediate the initial attachment and rolling (since bonds can break and form very quickly) while integrins are involved when firm, irreversible binding is desired (when a leukocyte has reached its chosen site of action). In the experimental study [19], the data points were acquired at the end of 2-h incubation time. Therefore, an inherent shortcoming of the approach described in this work is the extraction of kinetic rate constants from data acquired for a constant duration. The authors clearly recognize that time-dependent data are critically important to the extraction of equally important rate constants for this process.

The internalization and externalization rate constants for the two cell types were of the same order of magnitude which may indicate similar growth stages in the two cell types [20]. However, the internalization rate constant for the folate receptor in the pre-down-regulation phase was found to be significantly higher than those cited in the literature [34]. The internalization and the externalization rate constants obtained in this study also depend on the distribution of receptors on the cell surface as well as the ratio of internal to external folate receptor pools. Studies have shown that the rate of recycling is dependent on cholesterol, such that in normal cells recycling of GPI-anchored proteins is slower than transmembrane anchored proteins, but in cholesterol depleted cells the rates are more equivalent [34,40]. Since the folate receptor cycle is dependent on the growth requirement, targeting these drug carriers when the growth requirement is high will allow a large number of the drug carriers to be internalized by the target cells. In this work a linear dependence was assumed between intracellular folate concentration and receptor function to model the down-regulation of folate receptors after reaching the threshold in intracellular folate concentration (Eqs. 13 and 14 in Choice of parameters section). Although the current approximation for the

down-regulation phenomenon reasonably predicts the behavior observed for this system, the authors acknowledge that this may not be applicable to all folate receptor–ligand systems. A more rigorous model would take into account the intracellular folate cycle which begins with the polyglutamation of folic acid molecules and its analogues [41]. A recent study has suggested that homocysteine plays an important role in the translational upregulation of the folate receptor cycle by linking the folate metabolism to the coordinated upregulation of folate receptor [42].

The numbers of receptors per cluster for the two cells type also lie in the range reported in the literature [24,27,43]. Since the number of folate receptors per cluster may vary from cluster to cluster and also from cell to cell, the current model was developed on the basis of assuming an average value. Similarly the inter-cluster spacing was also approximated based on a uniform distribution of the clusters on the cell surface. A recent study on the distribution of GPI-anchored proteins on the surface of normal cells have suggested that a small but significant fraction (20–40%) of these proteins are present in clusters of nanometer size (~4–5 nm), each consisting of approximately 4 molecules while the rest are present as monomers on the cell surface [43]. Based on their reported folate receptor density of 150–750 molecules/ $\mu\text{m}^2$ , it is apparent that each carrier can occupy only one cluster based on the fraction of receptors clustered on the cell surface. The threshold concentration for KB cells was found to be an order of magnitude higher compared to C6 cells. Other studies have also shown higher uptake of folate conjugates into KB cells compared to other cell types [5].

As seen in Fig. 6, incubation time plays an important role in optimizing the drug carriers. The model predicts that liposomes containing fewer folic acid molecules are internalized more than liposomes containing higher number of folic acid molecules when the incubation time is increased. The majority of the experimental studies published in the literature is performed by determining the incubation time for the experiments based on identifying the time point at which the uptake reaches a steady state. Since the uptake rates are orders of magnitude slower compared to the binding rates, the kinetics of processes can be crucial in determining the end point of the experiment. In several experimental studies conducted, the incu-

bation time ranges from 4 to 6 h on the assumption that steady state is eventually reached. In most of these studies the number of folic acid molecules per liposomes ranged from 200–400 [2,22,29]. However, as shown here, steady state is not reached with these incubation times when the number of ligands per liposome is low. Thus one can achieve higher liposomal uptake at lower ligand numbers if the incubation time is increased. One may also reach a wrong conclusion on the optimal design of drug carrier if the kinetics of the process is not taken into consideration. A recent *in vivo* study on targeting of folate-bearing liposomes to tumor cells showed that targeting characteristics of drug carriers provided a 6 fold higher association of drug carriers with tumor cells compared to non-targeted carries [44]. However, since the circulation time of targeted drug carriers is lower compared to that of non-targeted carriers, it would become important to optimize the number of ligands per carriers so as to maximize intracellular drug delivery and increase circulation time.

As seen in Fig. 7, the effect of liposome concentration varies significantly only when the number of ligands per liposome is low. The curve plateaus out at higher liposome concentration even for low numbers of ligands per liposome. This likely happens due to the fact that the internalization process being slower than the binding of liposomes to cell surface, is the rate limiting step. Therefore, changing the concentration of drug carriers will not have a substantial effect on the overall uptake by tumor cells as the uptake is limited by both the binding and internalization of the drug carriers.

The current model developed is also based on the assumption that each liposome can interact with a single cluster of folate receptors. However, at very large number of cell surface receptors, the clusters may be closely spaced which results in the simultaneous binding of liposome to two or more clusters. Similarly if longer tethers are used, each liposome may be attached to more than one cluster. Another shortcoming of the model is that it does not take into account tether dynamics due to the flexibility of the polymer to which the ligand is attached. Tether dynamics will play a significant role in determining the number of bonds formed between ligands and receptors. An *ab-initio* calculation using an analytical model for tether dynamics based on self-consistent

field theory [45] suggests that a 2000 molecular weight PEG has a negligible probability of being more than 4 nm in length from the surface of the liposome. Thus, the number of receptor–ligand bonds that can be formed between a single liposome and cell surface is much lower compared to the current model which assumes every ligand in the AFAC as having the same probability of binding.

The length of the tether is also a consideration *in vivo*. The current model described in this paper and the experimental study only considered *in vitro* interactions. Thus, the only PEG species on the liposomes was the tether. Since a maximum of about 1000 ligands was used in this work, the maximum surface concentration of PEG conjugates was less than 1%. At this low level, inter-molecule entanglement does not occur, the PEG molecules are too far apart. Self-entanglement could occur, but is accounted for in the estimation of the binding distance described elsewhere [21]. *In vivo* however, it has shown that a stealth coating is required for ligand-targeted liposomes to have sufficient circulation time so as to be effective in delivering drug to the target site [2]. However, a stealth layer of the same molecular weight polymer as the ligand tether effectively shields the ligand from cell surface receptors, and prevents binding. Thus, a tether that is *longer* than the polymer of the stealth layer has to be used, effectively protruding the ligand above the stealth layer. In this situation, entanglement of the polymer chains is definitely possible. However, if one calculates an average length difference between the stealth layer and the tether length, this parameter can be substituted for tether length in the present model, thus accounting for the effect of the inter-molecule entanglement.

Although the mechanism of carrier–cell interactions are more complicated in *in vivo* systems, the current model provides a good starting point in the design of optimal drug formulations for *in vitro* studies. Current work in our group is focused on generalizing the model to study targeting of drug carriers to other receptor types as well. Several other receptors (e.g., transferrin receptors, LDL receptors, EGF receptor) found on the cell surface are either distributed in clusters or semi-heterogeneously distributed (i.e. clusters on a background of individually distributed receptors). In such cases, the number of drug carriers that can be internalized by the cell will depend on the number of drug carriers bound on the

cell surface. If the number of ligands per carrier is large or if the ligands are attached to long tethers, and if the clusters are sufficiently closely spaced, the carrier may bind to several clusters simultaneously. Occupation of multiple clusters by a single drug carrier could allow fewer drug carriers to bind to the surface which may result in low internalization efficiency. Finally, incorporating the dynamics of tether length and the uptake of drug carriers to tumor cells in the presence of healthy cells is also currently under investigation.

## 6. Conclusions

A deterministic population balance model was developed to study the interactions of ligand-bearing drug carriers with tumor cells *in vitro*. The model was able to predict the experimental data reasonably well for the system described here. The model also provides initial insights into the mechanism of interaction between targeted drug carriers and cell surface. In summary, knowledge of the distribution of receptors on the cell surface and their internalization pathway play a critical role in optimizing the drug carriers for intracellular delivery. For the specific case studied here, the overall uptake of ligand plays a crucial role in determining the uptake of carriers by the cells. Finally, the number of ligands per drug carrier and the length of tether are also important in determining the number of bonds a carrier can form with the cell surface.

## Acknowledgement

Funding for this research was provided by NSF BES 0401627 (RVB, AVA).

## References

- [1] D.A. Eavarone, X. Yu, R.V. Bellamkonda, Targeted drug delivery to C6 glioma by transferrin-coupled liposomes, *J. Biomed. Mater. Res.* 51 (2000) 10–14.
- [2] A. Gabizon, A.T. Horowitz, D. Goren, D. Tzemach, F. Mandelbaum-Shavit, M.M. Qazen, S. Zalipsky, Targeting folate receptor with folate linked to extremities of poly(ethylene glycol)-grafted liposomes: *in vitro* studies, *Bioconjug. Chem.* 10 (1999) 289–298.
- [3] A. Kurihara, Y. Deguchi, W.M. Pardridge, Epidermal growth factor radiopharmaceuticals: <sup>111</sup>In chelation, conjugation to a blood–brain barrier delivery vector via a biotin–polyethylene linker, pharmacokinetics, and *in vivo* imaging of experimental brain tumors, *Bioconjug. Chem.* 10 (1999) 502–511.
- [4] D.A. Lappi, Tumor targeting through fibroblast growth factor receptors, *Semin Cancer Biol.* 6 (1995) 279–288.
- [5] R.J. Lee, P.S. Low, Folate-mediated tumor cell targeting of liposome-entrapped doxorubicin *in vitro*, *Biochim. Biophys. Acta* 1233 (1995) 134–144.
- [6] S.K. Bhatia, M.R. King, D.A. Hammer, The state diagram for cell adhesion mediated by two receptors, *Biophys. J.* 84 (2003) 2671–2690.
- [7] C. Cozens-Roberts, D.A. Lauffenburger, J.A. Quinn, Receptor-mediated cell attachment and detachment kinetics: I. Probabilistic model and analysis, *Biophys. J.* 58 (1990) 841–856.
- [8] D.A. Hammer, D.A. Lauffenburger, A dynamical model for receptor-mediated cell adhesion to surfaces, *Biophys. J.* 52 (1987) 475–487.
- [9] C. Zhu, Kinetics and mechanics of cell adhesion, *J. Biomech.* 33 (2000) 23–33.
- [10] D.A. Lauffenburger, J.J. Linderman, *Receptors: Models for Binding, Trafficking, and Signaling*, Oxford University Press, New York, 1993.
- [11] A.S. Perelson, C. DeLisi, F.W. Wiegel, *Cell Surface Dynamics: Concepts and Models*, Marcel Dekker, New York, 1984.
- [12] J. Hubble, A model of multivalent ligand–receptor equilibria which explains the effect of multivalent binding inhibitors, *Mol. Immunol.* 36 (1999) 13–18.
- [13] J. Hubble, R. Eisenthal, W.J. Whish, A model for the initial phase of cell/surface interactions based on ligand binding phenomena, *Biochem. J.* 311 (1995) 917–919.
- [14] W.S. Hlavacek, R.G. Posner, A.S. Perelson, Steric effects on multivalent ligand–receptor binding: exclusion of ligand sites by bound cell surface receptors, *Biophys. J.* 76 (1999) 3031–3043.
- [15] D.J. Irvine, K.A. Hue, A.M. Mayes, L.G. Griffith, Simulations of cell-surface integrin binding to nanoscale-clustered adhesion ligands, *Biophys. J.* 82 (2002) 120–132.
- [16] N. Düzgünes, S. Nir, Mechanisms and kinetics of liposome–cell interactions, *Adv. Drug Deliv. Rev.* 40 (1999) 3–18.
- [17] K.D. Lee, S. Nir, D. Papahadjopoulos, Quantitative analysis of liposome–cell interactions *in vitro*: rate constants of binding and endocytosis with suspension and adherent J774 cells and human monocytes, *Biochemistry* 32 (1993) 889–899.
- [18] T.J. English, D.A. Hammer, Brownian adhesive dynamics (BRAD) for simulating the receptor-mediated binding of viruses, *Biophys. J.* 86 (2004) 3359–3372.
- [19] J.M. Saul, A. Annappagada, J.V. Natarajan, R.V. Bellamkonda, Controlled targeting of liposomal doxorubicin via the folate receptor *in vitro*, *J. Control. Release* 92 (2003) 49–67.
- [20] M.M. Doucette, V.L. Stevens, Folate receptor function is regulated in response to different cellular growth rates in cultured mammalian cells, *J. Nutr.* 131 (2001) 2819–2825.
- [21] C. Jeppesen, J.Y. Wong, T.L. Kuhl, J.N. Israelachvili, N. Mullah, S. Zalipsky, C.M. Marques, Impact of polymer tether

- length on multiple ligand–receptor bond formation, *Science* 293 (2001) 465–468.
- [22] R.J. Lee, P.S. Low, Delivery of liposomes into cultured KB cells via folate receptor-mediated endocytosis, *J. Biol. Chem.* 269 (1994) 3198–3204.
- [23] K. Jacobson, C. Dietrich, Looking at lipid rafts? *Trends Cell Biol.* 9 (1999) 87–91.
- [24] S. Mayor, R. Varma, GPI-anchored proteins are organized in submicron domains at the cell surface, *Nature* 394 (1998) 798–801.
- [25] E.D. Sheets, G.M. Lee, R. Simson, K. Jacobson, Transient confinement of a glycosylphosphatidylinositol-anchored protein in the plasma membrane, *Biochemistry* 36 (1997) 12449–12458.
- [26] S. Sabharanjak, P. Sharma, R.G. Parton, S. Mayor, GPI-anchored proteins are delivered to recycling endosomes via a distinct cdc42-regulated, clathrin-independent pinocytic pathway, *Dev. Cell Biol.* 2 (2002) 411–423.
- [27] T. Friedrichson, T.V. Kurzchalia, Microdomains of GPI-anchored proteins in living cells revealed by crosslinking, *Nature* 394 (1998) 802–805.
- [28] J. Wang, W. Gunning, K.M. Kelley, M. Ratnam, Evidence for segregation of heterologous GPI-anchored proteins into separate lipid rafts within the plasma membrane, *J. Membr. Biol.* 189 (2002) 35–43.
- [29] J. Sudimack, R.J. Lee, T. Lee, W.J. Guo, Receptor-specific delivery of liposomes via folate–PEG–Chol, *J. Liposome Res.* 10 (2000) 179–195.
- [30] W.S. Hlavacek, C. Wofsy, A.S. Perelson, Dissociation of HIV-1 from follicular dendritic cells during HAART: mathematical analysis, *Proc. Natl. Acad. Sci. U. S. A.* 96 (1999) 14681–14686.
- [31] B.A. Kamen, M.T. Wang, A.J. Streckfuss, X. Peryea, R.G. Anderson, Delivery of folates to the cytoplasm of MA104 cells is mediated by a surface membrane receptor that recycles, *J. Biol. Chem.* 263 (1988) 13602–13609.
- [32] C.P. Leamon, P.S. Low, Delivery of macromolecules into living cells: a method that exploits folate receptor endocytosis, *Proc. Natl. Acad. Sci. U. S. A.* 88 (1991) 5572–5576.
- [33] B.A. Kamen, A. Capdevila, Receptor-mediated folate accumulation is regulated by the cellular folate content, *Proc. Natl. Acad. Sci. U. S. A.* 83 (1986) 5983–5987.
- [34] S. Mayor, S. Sabharanjak, F.R. Maxfield, Cholesterol-dependent retention of GPI-anchored proteins in endosomes, *Embo J.* 17 (1998) 4626–4638.
- [35] P.N. Brown, G.D. Byrne, A.C. Hindmarsh, VODE, a variable-coefficient ODE solver, *SIAM Journal on Scientific and Statistical Computing* 10 (1989) 1038–1051.
- [36] J.A. Reddy, C. Abburi, H. Hofland, S.J. Howard, I. Vlahov, P. Wils, C.P. Leamon, Folate-targeted, cationic liposome-mediated gene transfer into disseminated peritoneal tumors, *Gene Ther.* 9 (2002) 1542–1550.
- [37] M. McHugh, Y.C. Cheng, Demonstration of a high affinity folate binder in human cell membranes and its characterization in cultured human KB cells, *J. Biol. Chem.* 254 (1979) 11312–11318.
- [38] J.J. Turek, C.P. Leamon, P.S. Low, Endocytosis of folate–protein conjugates: ultrastructural localization in KB cells, *J. Cell Sci.* 106 (1993) 423–430.
- [39] O.A. Eniola, P.J. Willcox, D.A. Hammer, Interplay between rolling and firm adhesion elucidated with a cell-free system engineered with two distinct receptor–ligand pairs, *Biophys. J.* 85 (2003) 2720–2731.
- [40] W.J. Chang, K.G. Rothberg, B.A. Kamen, R.G. Anderson, Lowering the cholesterol content of MA104 cells inhibits receptor-mediated transport of folate, *J. Cell Biol.* 118 (1992) 63–69.
- [41] A.C. Antony, The biological chemistry of folate receptors, *Blood* 79 (1992) 2807–2820.
- [42] A.C. Antony, Y.S. Tang, R.A. Khan, M.P. Biju, X. Xiao, Q.J. Li, X.L. Sun, H.N. Jayaram, S.P. Stabler, Translational upregulation of folate receptors is mediated by homocysteine via RNA–heterogeneous nuclear ribonucleoprotein E1 interactions, *J. Clin. Invest.* 113 (2004) 285–301.
- [43] P. Sharma, R. Varma, R.C. Sarasij, Ira, K. Gousset, G. Krishnamoorthy, M. Rao, S. Mayor, Nanoscale organization of multiple GPI-anchored proteins in living cell membranes, *Cell* 116 (2004) 577–589.
- [44] A. Gabizon, A.T. Horowitz, D. Goren, D. Tzemach, H. Shmeeda, S. Zalipsky, In vivo fate of folate-targeted polyethylene–glycol liposomes in tumor-bearing mice, *Clin. Cancer Res.* 9 (2003) 6551–6559.
- [45] C.M. Wijmans, E.B. Zhulina, Polymer brushes at curved surfaces, *Macromolecules* 26 (1993) 7212–7224.